Hindawi
Mathematical Problems in Engineering
Volume 2019, Article ID 8015295, 9 pages
https://doi.org/10.1155/2019/8015295

Research Article

An Improved Empirical Mode Decomposition Method Using Variable Window Median Filter for Early Fault Detection in Electric Motors

Erinc Karatoprak and Serhat Seker

Faculty of Electrical and Electrical Engineering, Istanbul Technical University, Istanbul, Turkey

Correspondence should be addressed to Erinc Karatoprak; karatoprak@gmail.com

Received 14 December 2018; Accepted 4 February 2019; Published 19 February 2019

Academic Editor: Fazal M. Mahomed

This paper proposes an improved Empirical Mode Decomposition (EMD) method by using variable window size median filters during the Intrinsic Mode Functions (IMFs) generation. Compared to the traditional EMD, the improved EMD, namely, Median EMD (MEMD), helps to reduce mode-mixing providing an improvement in terms of separating the fundamental frequencies per IMF. The MEMD method applies the EMD to the signal and then applies a variable window size median filter to the resulting IMFs. A narrow window is used for high frequency components where a broader window is used for the lower frequency components. The filtered IMFs are then summed again and another round of EMD is applied to yield the improved MEMD IMFs. A test setup for accelerated aging of bearings in induction motors is used for the comparison of the traditional and the improved EMD methods with the goal of finding potential bearing defects in an induction motor. The potential defect at the early stage is compared with the faulty state and is used to extract the characteristics of the bearing damage that develops gradually. Comparing the EMD and MEMD, it is seen that MEMD is an improvement to EMD in terms of mode-mixing problem. The MEMD method demonstrated to have better performance compared to the traditional EMD for the extraction of the fault features from the healthy operational state of the motor.

1. Introduction

Empirical Mode Decomposition (EMD) is a signal analysis method with a wide range of applications such as bearing fault detection, biomedical data analysis, power signal analysis, and seismic signals [1–6]

Although EMD has a wide area of applications, there are still issues related to the method that needs to be addressed such as mode mixing, end-effect, and spline problems [4].

When the EMD cannot successfully decompose the signal into unique frequency components, then different Intrinsic Mode Functions (IMF) contain the same frequencies as overlapping components. This is known as the mode mixing issue [4]. Another problem related to the EMD is the so-called end-effect[4], where large deviations occur in the interpolation fitting process of EMD resulting in the propagation and corruption of the data span [7].

There are various methods proposed to overcome these problems such as "B-spline EMD" [8], "mask signal improved EMD" [9], "adaptively fast ensemble empirical mode decomposition"[10], "improved CEEMD (Complete Ensemble EMD)" [11], and wavelet packet denoising improved EMD [12].

In this paper, a new method is proposed, i.e., the EMD improved with median filtering which provides a filter that eliminates the effects of the impulse noise while decreasing the mode-mixing. Median filter in general allows eliminating the impulse noise in various different signal analysis applications [13]. In the MEMD method, a variable window sized median filter is applied to the IMFs.

Firstly, EMD is applied to the signal to generate the IMFs. A variable window sized median filter is applied to these IMFs, where a narrow window size is used for high frequency components and a broader window size is used for low

frequency components. These filtered IMFs are then summed to reconstruct the signal. EMD is once again applied to the reconstructed signal and the improved IMFs are generated. Comparison of the results of the MEMD and the regular EMD shows that the new method, i.e., MEMD, improves the decomposition in terms of mode mixing, allowing a better decomposition of the each frequency component per IMF.

Section 2 describes the regular EMD method while the improved EMD and the median filter are explained in section 3. The details of how to arrange the variable window size and how to reconstruct the signal after the filtering are also explained in section 3. Also a flowchart diagram is given to provide a clear understanding of the whole process. In section 4, the electric motor aging setup and process are explained. In section 5, the data from healthy and faulty motors are compared with the improved and the regular EMD method and the corresponding results are discussed.

Section 6 summarizes the results of the improved EMD and the possible improvement points for further clarifying the window size selection criteria and the further potential use of this method in a classification algorithm.

2. Empirical Mode Decomposition

EMD is an adaptive signal analysis method that allows decomposing the signal into different frequency components [14]. These components are called Intrinsic Mode Functions (IMFs). The two conditions that need to be satisfied for a component to be considered an IMF are the following [15]:

(i) Total zero crossings and the total extrema in the whole data set should be equal or vary by at most one.

(ii) The mean value of envelope from maxima and minima should be equal to zero at any interval of the component.

EMD can decompose any signal into IMFs. EMD is a sifting process with the goal of decomposing the signal into narrow band signals.

The EMD/sifting process can be explained as follows:

(1) Identify all the local minima and maxima.

(2) Connect all the local maxima/minima by a cubic spline to form the upper/lower envelope.

(3) Calculate the mean of these envelops m_1 and subtract it from the signal $h_1 = x(t) - m_1$.

(4) Check if h_1 satisfies the two criteria for IMF. If not repeat steps through 1 to 3 until h satisfies the IMF criteria.

Assuming after i times of iteration, the conditions are satisfied:

$$h_{1(i-1)} - m_{1i} = h_{1i};$$
$$\text{then } c_1 = h_{1i} \text{ becomes the first IMF.} \tag{1}$$

The most widely used stoppage criteria for the number of iterations are explained by Huang et al. [15, 16] which are given by a Cauchy convergence test; normalized squared difference between two consecutive sifting must be smaller than a certain value.

The first IMF is expected to contain the high frequency oscillations in the signal [5].

$$x(t) - c_1 = r_1 \tag{2}$$

The residue r_1 contains all the remaining frequency information of the data and is treated as the signal and another sifting process is applied to produce the second IMF c_2.

$$\begin{aligned} r_1 - c_2 &= r_3 \\ r_{n-1} - c_n &= r_n \end{aligned} \tag{3}$$

This process stops when the residue r_n is a monotonic function or a function with only one extremum; thus no additional IMF can be extracted as by definition [16].

Thus the function can be displayed as

$$x(t) = \sum_{i=1}^{I} \left(c_i(t) + r_I(t)\right) \tag{4}$$

where $c_i(t)$ is the ith IMF and $r_I(t)$ is the residual signal.

3. Median Empirical Mode Decomposition

In the MEMD method, the signal is decomposed into IMFs and then a variable window sized median filter is applied to each IMF component. Afterwards, these IMFs are summed again to recompose the signal. The recomposed signal is again decomposed by EMD and the improved IMFs are created.

3.1. Median Filter. The nonlinear median filter enables removing noise and smoothening a signal. The function of a median filter can be given as [17]

$$\begin{aligned} &y(t) = median\left[x(t-l), x(t-l+1) \cdots x(n)\right. \\ &\quad \left. \cdots x(t+l-1), x(t+l)\right] \\ &x(t);\ Input\ signal \\ &y(t);\ Output\ signal \end{aligned} \tag{5}$$

The filter goes through the signal point by point and replaces each input with the median of its neighbors [17]. This concept of neighbors can be defined as a sliding "window" which indeed slides per each input over the entire signal. For a single-dimension signal, the window can be taken as a certain number of preceding and following entries of the point [18].

The median filter with a small window size eliminates most of the noise but also results in the loss of some information whereas a large window sized median filter does the opposite: less information loss; however also less noise filtering [19].

3.2. MEMD with Median Filter. Once EMD is applied to the original signal, the signal is decomposed into IMFs (different

frequency components). Since each IMF contains the different frequency components of the original data, applying a median filter with variable window size can provide better results in terms of handling different frequency bands. For high frequency IMFs a smaller window sized median filter is applied whereas the window size is increased for the lower frequency IMFs. These variable window median filters allow eliminating noise in high frequency components while keeping the information of lower frequency components intact [20, 21].

The window size of the median filter increases with the order of IMFs. The smaller the order of the IMF is, the smaller the window size is chosen. The window size selection is explained later in this section.

Once all the IMFs are generated and the relevant median filtering is applied for each IMF, these median filtered IMFs out of the regular EMD process are summed together to generate the filtered version of the original data.

At this point, EMD process is again applied to the filtered version of the original data and new IMFs are generated.

The process consists of the following steps.

Step 1. Apply EMD algorithm to the signal $x(t)$ and get the IMF components $c_l(t)$ and the residue $r(t)$ where $l = 1, 2, \ldots L$, the number of IMFs. Normalize all the IMFs.

Step 2. Use the window size *hf* for the IMFs defined to be high frequency and use the window size *lf* for the rest of the IMFs to produce the median filtered IMFs $c_{med,l}(t)$

Step 3. Sum all the median filtered IMFs $c_{med,l}(t)$ to create the filtered version of the original signal, i.e., $x_{filtered}(t)$.

Step 4. Apply the EMD algorithm on $x_{filtered}(t)$ to generate the improved IMFs $d_m(t)$ where $m = 1, 2, \ldots M$ is the number of improved IMFs

The window size of the median filter increases with the order of IMFs. A smaller window size is chosen for the initial IMFs, where window size grows for the latter IMFs. To realize this, two adaptive windows are defined, where the "high frequency" IMFs are filtered with the smaller window and the rest with the larger window size.

Once the initial EMD process is completed and the IMFs are generated, the dominant frequency of each IMF is checked, i.e., the frequency band that carries the most energy. If L is the number of IMFs, then the following fundamental frequencies are available:

$$f_{IMF1}, f_{IMF2}, \ldots, f_{IMFL} \tag{6}$$

An IMF is considered to be high frequency if the fundamental frequency of that IMF is higher than the half of the highest frequency IMF plus the lowest frequency IMF.

Fundamental High frequency – Low frequency criteria point:

$$f_{IMFi} \leq \frac{f_{IMF1}}{2} + f_{IMFL} : \textit{Low Frequency IMF}$$
$$f_{IMFi} > \frac{f_{IMF1}}{2} + f_{IMFL} : \textit{High Frequency IMF} \tag{7}$$

Based on the above decision point, IMFs are classified as high frequency and low frequency. All IMFs from i to L including i would be processed as low frequency, whereas all IMFs from 1 to i would be processed as high frequency IMFs.

The below window sizes are applied for each IMF based on them being high or low frequency.

High frequency window size for the i^{th} IMF can be given as

$$hf = round\left(\frac{i}{L} * H\left(IMF_i\right)\right) \tag{8}$$

Low frequency window size for the i^{th} IMF can be given as

$$lf = round\left(\frac{i}{L} * \left(H\left(IMF_i\right)\right)^2\right)$$
$$L\text{: The number of IMFs} \tag{9}$$
$$H\left(IMF_i\right)\text{: Shannon entropy of the } IMF_i$$

The Shannon entropy of the IMF is calculated based on [22]

$$H\left(p\right) = -\sum_{i=1}^{k} p\left(i\right) \log\left(p\left(i\right)\right) \tag{10}$$

The above criteria on how to calculate the window size for median filter allow creating a unique median filter with a unique window size per each IMF. The method links each window size with the whole data by means of using the number of the IMFs; moreover it also links the window size with each IMF itself via the entropy of that given IMF.

A fixed window size per IMF [21] provides a means to improve the data by removing as much impulse noise as possible, whereas this new method applied in MEMD additionally provides a direct connection between the entropy of each IMF and the window size for the median filter. As it will be explained further within this paper as part of the experiment and the analysis, this new method does not only help to eliminate noise and improve mode-mixing [21], but also allows a clear distinction of physically meaningful frequency components of the data.

The flowchart of the whole process is shown in Figure 1.

4. Accelerated Aging and Bearing Damage

4.1. Experimental Setup and Data Acquisition System. A test setup is designed to simulate the electrical discharge from the shaft to the bearing [23–25]. This test setup, Electrical Discharge Machining (EDM), can be seen in Figure 2. The motor was run at no load for 30 minutes for each cycle with an external shaft current of 27 Amperes at 30 Volts AC [24, 25]

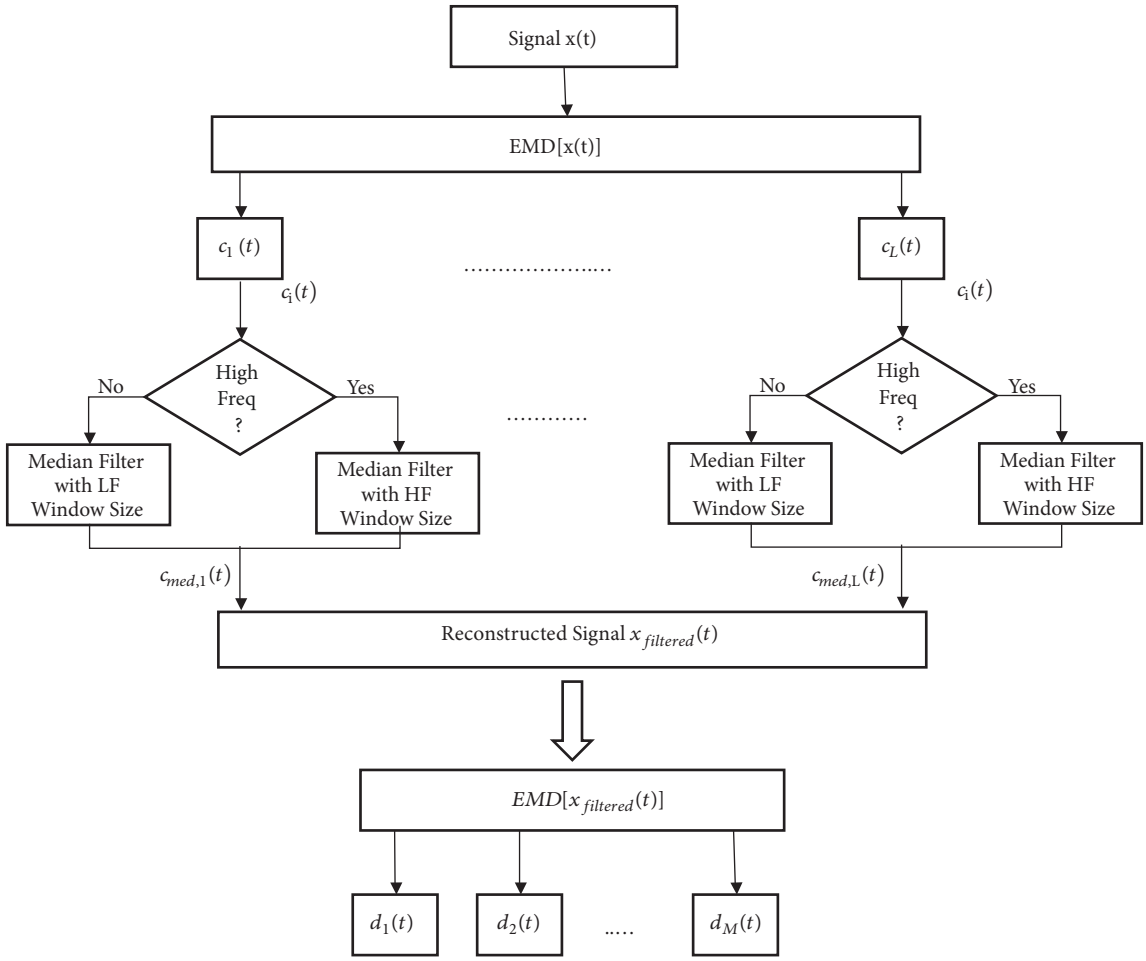

Figure 1: The flowchart of the algorithm.

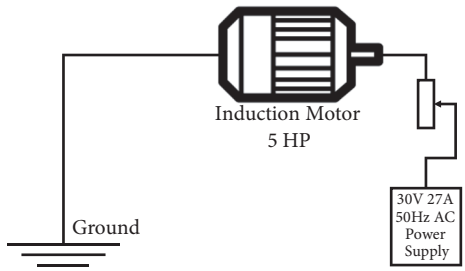

Figure 2: EDM test setup.

Acceleration of the aging process is realized by applying thermal aging after each cycle of EDM aging. The aging of the motor is realized in cycles, where each cycle includes an EDM and thermal aging process. After each cycle of accelerated aging, the motor was run on a performance test platform [24, 25]. During the performance test, current, voltage, rotor speed, torque, and vibration data were collected from the motor with a sampling frequency of 12 kHz.

In total there were 8 cycles, where cycle 0 was the healthy operational state of the motor and cycle 7 was the faulty case.

Figure 3 shows the performance test setup used after each accelerated aging process where the data collection on the motor is done. There are in total six accelerometers used for different vibration measurements. The sensors S1 and S2 (in plane A-B) are identical and provide the most significant data in terms of bearing damage [23–25]. Thus, Sensor S-1 is chosen for the analysis. As the aging progresses, the vibration amplitude increases [23].

In order to analyze the data, Power Spectral Density (PSD) graphs are referred. The PSD of a signal shows the distribution of power per each frequency component of that signal [26].Figures 4 and 5 show the PSD of the healthy and faulty states of the motor.

The PSD of the healthy state of the motor in Figure 4 shows frequency components around 2.5 kHz with very low amplitude.

The PSD of the faulty state of the motor in Figure 5 shows that those frequency components around 2.5 kHz are greatly increased in amplitude. These frequency components around the range of 2.5 kHz are known to be the characteristics of the fault [23].

By comparing Figures 4 and 5, it is important to note that the fault related frequencies (~ 2.5 kHz) [23] are already

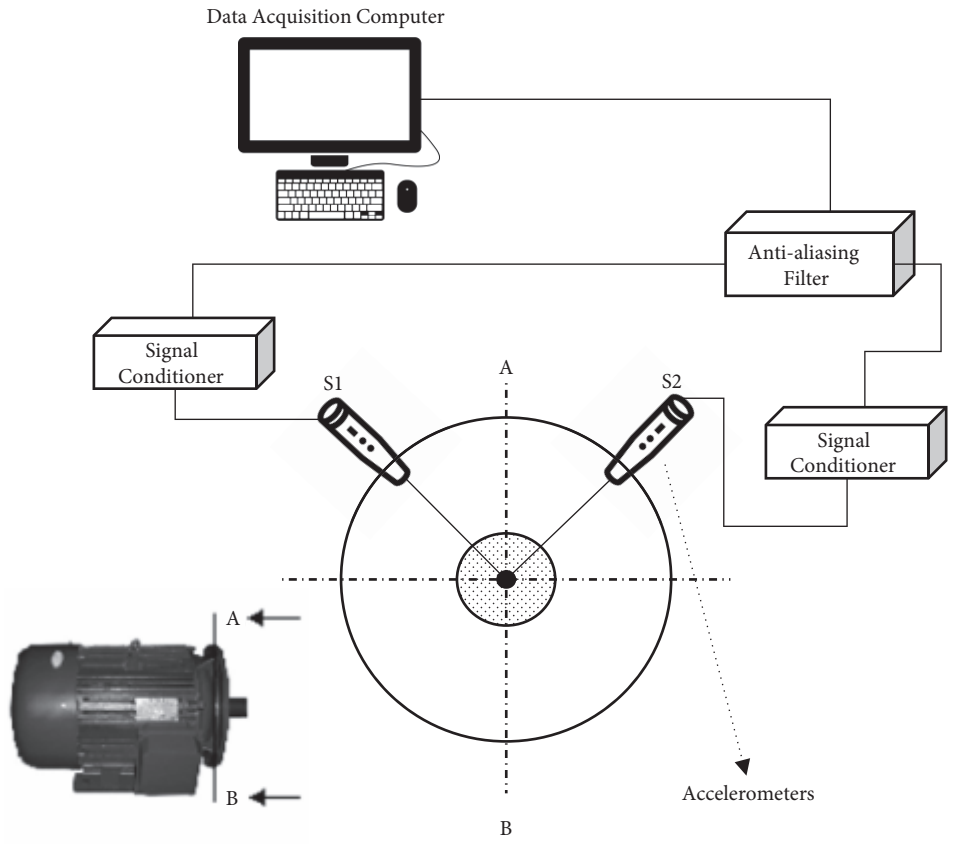

Figure 3: Motor performance test and data acquisition setup.

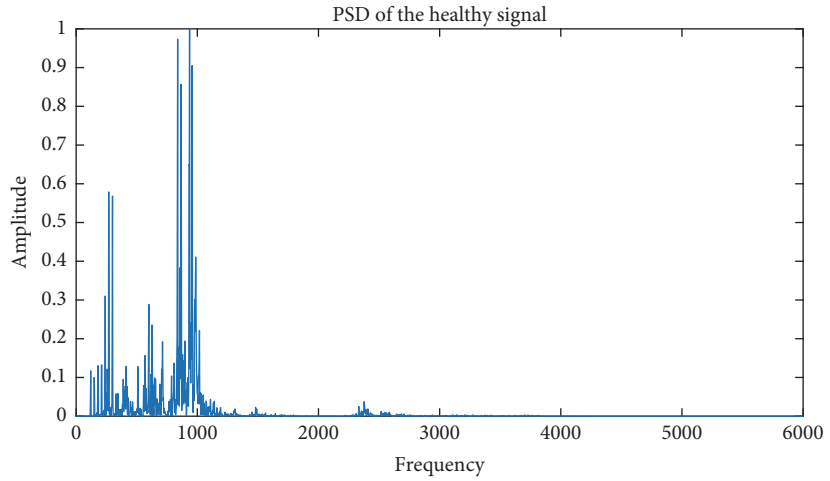

Figure 4: The PSD of the healthy motor.

available in the healthy motor (Figure 4) with a relatively very low amplitude and as the degradation of the bearing progresses, these components around 2.5 kHz become more visible in the frequency spectrum.

5. MEMD Method for Early Fault Detection

The data gathered from the healthy state of the motor is analyzed by both EMD and the MEMD method.

Figures 6 and 7 show that there is a big difference between the 1st IMF of EMD and the MEMD. In MEMD, the high frequency components on the neighborhood of 2.5 kHz are filtered as a separate component. The MEMD method shows the components with the ~ 1kHz frequency range as a second IMF. However the EMD method mixes those ~2.5 kHz components with the ~1 kHz frequency range components and fails to distinguish these two different physical facts.

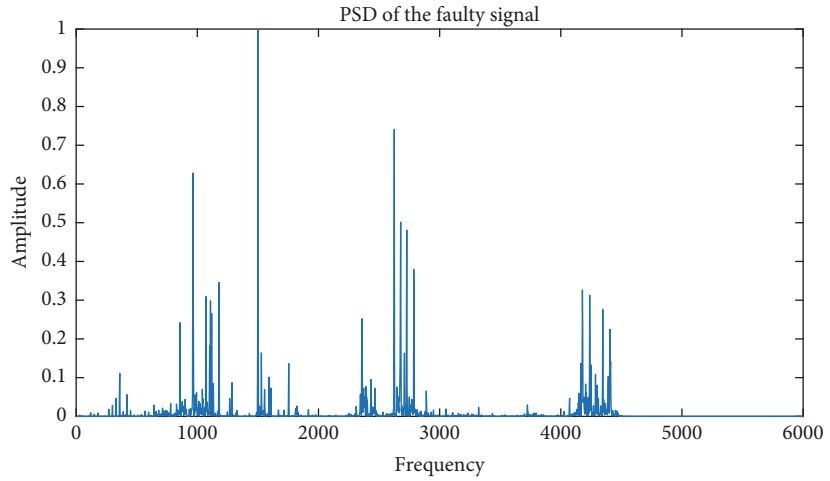

Figure 5: The PSD of the faulty motor.

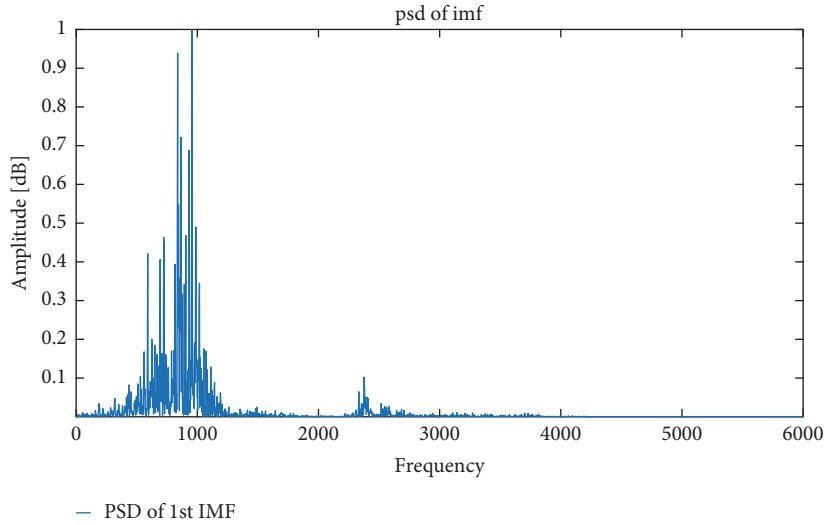

Figure 6: The 1st IMF of the EMD for the healthy motor.

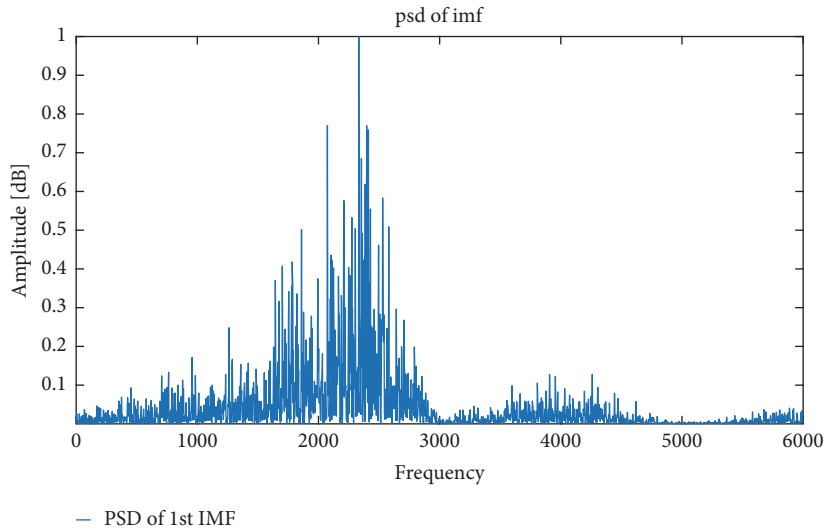

Figure 7: The 1st IMF of the MEMD for the healthy motor.

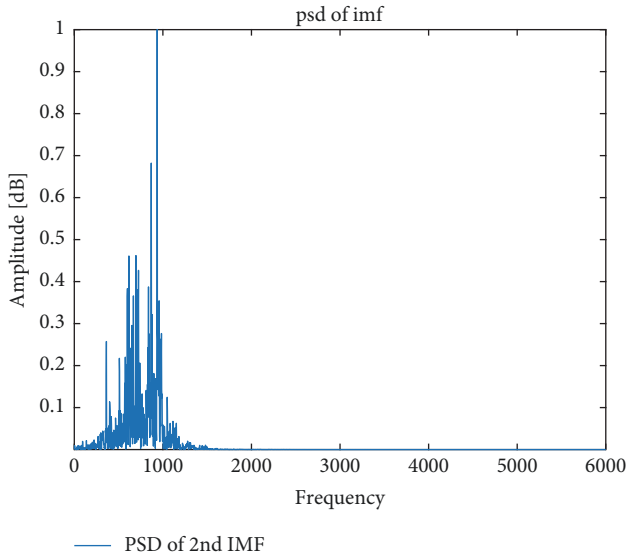

Figure 8: The 2nd IMF of the EMD for the healthy motor.

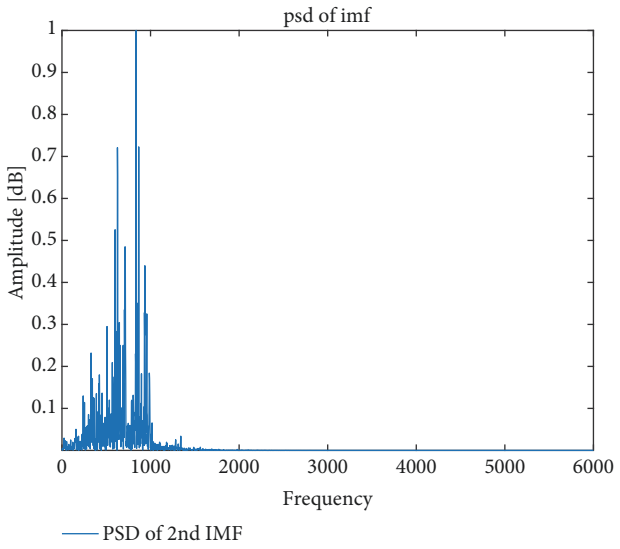

Figure 9: The 2nd IMF of the MEMD for the healthy motor.

The physical meaning of this is that the very low amplitude fault frequencies are recognized as a separate component, instead of summing them together with the 1 kHz components. This is made possible by the median filter, where the filtering softens the high amplitude components of the lower frequencies, thus providing the possibility for EMD to be able to decompose this underlying physical fact as a separate component. In other words, the filtering allowed EMD method to catch these very low amplitude high frequency components (~ 2.5 kHz) in the presence of the lower frequency components with the much higher amplitude values. This fact is also fully in line with the physical properties of the system [23].

Figure 8 shows the 2nd IMF for the regular EMD method. By checking the 1st and 2nd IMFs of the original EMD method, respectively, Figures 6 and 8, it is seen that there is a considerable amount of mode mixing present on the 1 kHz frequency range. Both 1st and 2nd IMF of the regular EMD represent the same physical components while missing the fault features as a separate component.

It is interesting to note that the 2nd IMF of MEMD method, as seen in Figure 9, successfully represents the 1 kHz range physical component with relatively little mode mixing. Briefly, the information represented in the 1st IMF of the regular EMD method is successfully divided into two in the MEMD method as shown in Figures 7 and 9, and the 1st MEMD IMF represents the fault frequencies, which means the physical impact of the degradation can already be identified as a feature/component which can be monitored for the degradation.

Briefly, the 1st and 2nd IMF of the regular EMD method show a mix of components (the 1 kHz range and the 2.5 kHz range), while the MEMD method clearly separates these two different physical facts into two different IMFs.

The MEMD method's contribution is that it successfully distinguishes the physically meaningful fault frequency components that are already available in the initial healthy state measurements with very low amplitude, while the regular EMD method fails in this and can only distinguish these components when the fault is already present.

While the method was able to distinguish this physical fact, it did not have a significant success in the lower frequency ranges in terms of distinguishing more detailed physically meaningful frequency components compared to the traditional EMD method. This limitation would require further study and analysis in order to provide an improvement on the lower frequency range as well.

6. Conclusion

In this paper, a median filter based MEMD method is described and compared with the EMD method. It is shown that the MEMD method which has adaptive window sized median filter provides an improvement for the mode-mixing problem by noise filtering and by allowing the data to be decomposed into physically meaningful components that were not separable previously.

Data from the induction machine rolling bearing fault is used to compare the MEMD and EMD methods. MEMD method is successful in distinguishing the very low amplitude frequencies related to the fault at the healthy state, whereas the EMD method failed in doing so.

The first IMF of the traditional EMD method shows the fault related frequencies mixed with the frequencies of the operation of the motor and is not able to distinguish them. On the contrary, the improved MEMD method shows these fault related higher frequencies as the 1st IMF, while the operational frequencies are pushed to the 2nd IMF. This shows that the improved MEMD method is able to decompose the data into physically meaningful frequency components. Figure 10 shows the comparison of the 1st IMF for both improved and the traditional EMD methods and Figure 11

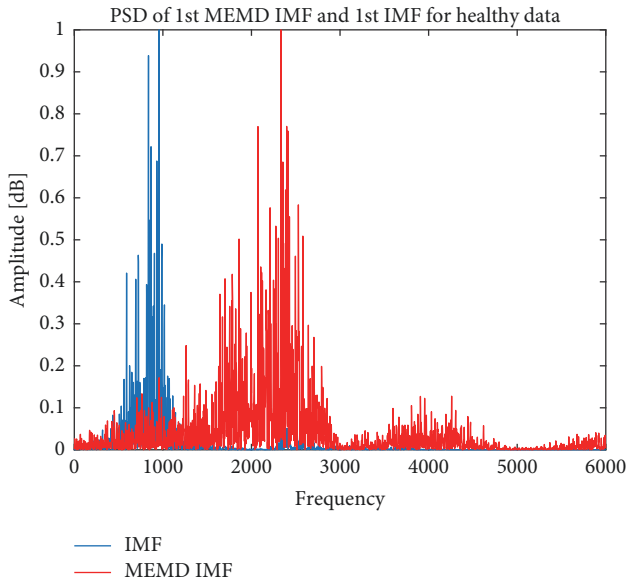

Figure 10: Comparison of the PSD for the 1st IMF of EMD and MEMD for healthy data.

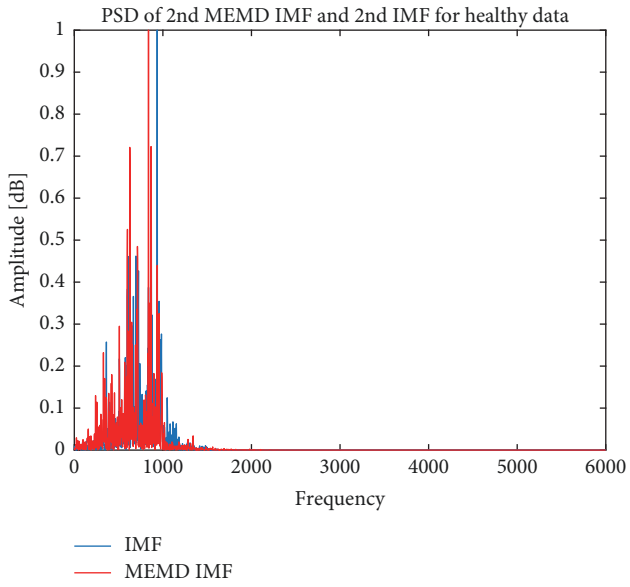

Figure 11: Comparison of the PSD for the 2nd IMF of EMD and MEMD for healthy data.

shows the comparison of the 2nd IMF for both improved MEMD and the traditional EMD methods.

In terms of improving the MEMD method further, it would be beneficial to do further analysis and research on the median filter size selection and its relation with the frequency components of the IMFs on the lower frequencies to improve the decomposition for low frequency components as well.

The success of the MEMD allows it to be used as a feature extraction method where the physically meaningful frequencies can be distinguished at the normal/healthy operating state and be monitored as part of a real-time condition monitoring system for fault detection.

Data Availability

The data used to support the findings of this study are available from the corresponding author upon request.

Conflicts of Interest

The authors declare that there are no conflicts of interest regarding the publication of this paper.

Acknowledgments

The authors have not received any funding for this study.

References

[1] Y. Lei, J. Lin, Z. He, and M. J. Zuo, "A review on empirical mode decomposition in fault diagnosis of rotating machinery," *Mechanical Systems and Signal Processing*, vol. 35, no. 1-2, pp. 108–126, 2013.

[2] G. Goel and D. Hatzinakos, "Ensemble empirical mode decomposition for time series prediction in wireless sensor networks," in *International Conference of Computing, Networking and Communications (ICNC)*, pp. 594–598, IEEE, February 2014.

[3] V. K. Mishra, V. Bajaj, A. Kumar, and G. K. Singh, "Analysis of ALS and normal EMG signals based on empirical mode decomposition," *IET Science, Measurement & Technology*, vol. 10, no. 8, pp. 963–971, 2016.

[4] N. E. Huang, *Hilbert-Huang Transform And Its Applications*, vol. 16, World Scientific, 2014.

[5] A. Oztuerk and S. Seker, "On the Frequency Resolution of Improved Empirical Mode Decomposition Method," vol. 5, 2010.

[6] H. Liu, X. Wang, and C. Lu, "Rolling bearing fault diagnosis under variable conditions using hilbert-huang transform and singular value decomposition," *Mathematical Problems in Engineering*, vol. 2014, Article ID 765621, 8 pages, 2014.

[7] M. Feldman, "Hilbert transform in vibration analysis," *Mechanical Systems and Signal Processing*, vol. 25, no. 3, pp. 735–802, 2011.

[8] H. Li, C. Wang, and D. Zhao, "An improved EMD and its applications to find the basis functions of EMI signals," *Mathematical Problems in Engineering*, vol. 2015, Article ID 150127, 8 pages, 2015.

[9] R. Deering and J. F. Kaiser, "The use of a masking signal to improve empirical mode decomposition," in *Proceedings of the Acoustics, Speech, and Signal Processing (ICASSP'05)*, vol. 4, pp. iv–485, IEEE International, 2005.

[10] X. Xue, J. Zhou, Y. Xu, W. Zhu, and C. Li, "An adaptively fast ensemble empirical mode decomposition method and its applications to rolling element bearing fault diagnosis," *Mechanical Systems and Signal Processing*, vol. 62, pp. 444–459, 2015.

[11] M. Li, H. Wang, G. Tang, H. Yuan, and Y. Yang, "An improved method based on CEEMD for fault diagnosis of rolling bearing," *Advances in Mechanical Engineering*, vol. 6, Article ID 676205, 2014.

[12] X. U. Xin and P. A. N. Hongxia, "Study on the application of improved emd in gearbox fault diagnosis," *Journal of Mechanical Transmission*, vol. 10, pp. 4–8, 2014.

[13] Z. M. Ramadan, "A New method for impulse noise elimination and edge preservation," *Canadian Journal of Electrical and Computer Engineering*, vol. 37, no. 1, pp. 2–10, 2014.

[14] N. E. Huang, Z. Shen, S. R. Long et al., "The empirical mode decomposition and the Hilbert spectrum for nonlinear and non-stationary time series analysis," in *Proceedings of the In Proceedings of the Royal Society of London A: mathematical*, vol. 454, pp. 903–995, No, 1998.

[15] N. E. Huang and Z. Wu, "A review on Hilbert-Huang transform: method and its applications to geophysical studies," *Reviews of Geophysics*, vol. 46, no. 2, Article ID RG2006, 2008.

[16] N. E. Huang, M. L. C. Wu, S. R. Long et al., "A confidence limit for the empirical mode decomposition and Hilbert spectral analysis," in *Proceedings of The Royal Society of London A: Mathematical, Physical And Engineering Sciences*, vol. 459, pp. 2317–2345, The Royal Society, 2003.

[17] G. R. Arce, *Nonlinear Signal Processing A Statistical Approach*, John Wiley & Sons, New York, NY, USA, 2005.

[18] H. Azhari, *Basics of Biomedical Ultrasound for Engineers*, John Wiley & Sons, 2010.

[19] I. Pitas and A. N. Venetsanopoulos, *Nonlinear Digital Filters: Principles And Applications*, vol. 84, Springer Science & Business Media, 2013.

[20] C. T. Lu, Y. Y. Chen, L. L. Wang, and C. F. Chang, "Removal of salt-and-pepper noise in corrupted image using three-values-weighted approach with variable-size window," *Pattern Recognition Letters*, vol. 80, pp. 188–199, 2016.

[21] V. K. Mishra, V. Bajaj, A. Kumar, D. Sharma, and G. K. Singh, "An efficient method for analysis of EMG signals using improved empirical mode decomposition," *AEÜ - International Journal of Electronics and Communications*, vol. 72, pp. 200–209, 2017.

[22] C. E. Shannon, "A mathematical theory of communication," *Bell Labs Technical Journal*, vol. 27, pp. 379–423, 1948.

[23] S. Seker and E. Ayaz, "A study of condition monitoring for induction motors under accelerated aging process," *IEEE Power Engineering Review*, vol. 22, no. 7, pp. 35–37, 2002.

[24] IEEE Std 117-1974, *IEEE Standard Test Procedure for Evaluation of Systems of Insulation Materials for Random-Wound Ac Electric Machinery*, 1991.

[25] E. Karatoprak, T. Hengüler, E. Ayaz, and S. Heker, "Comparisons of the continuous and discrete wavelet transforms for pote ntial failure detection in electric motors," in *ELECO 5th International Conference on Electrical and Electronics Engineering*, 2007.

[26] P. Stoica and R. L. Moses, *Spectral Analysis of Signals*, 2005.